EXPERIMENTAL ANALYSIS OF THE OMNIDIRECTIONAL EXPLOSIVE DEVICES USED TO NEUTRALIZE IED

Alexandru Cătălin CASAPU [1], Marin LUPOAE [2 *], Eugen TRANĂ[3], Costin Dumitru BERECHET[4]

Improvised Explosive Devices (IEDs) have become a prevalent tool for terrorists in asymmetric warfare. Because of their simplicity and ease of use, explosive water jet propulsion devices are among the most commonly used tools for IED neutralization. This study investigates high-speed water jets generated by explosive charges as a remote neutralization technique applied to IED casings. Experimental evaluations focused on three materials - wood, metal, and polycarbonate - to analyze differences in structural disruption. Measurements included jet velocity at operational distances, overall disruption performance, and the initiation of blasting caps. The experimental tests offer preliminary insights into the interaction between water jets generating using omnidirectional system and various casing materials, contributing to the development of more efficient counter-IED devices. The results encourage continued innovation and rigorous analysis to enhance remote neutralization methods.

Keywords: casing materials, omnidirectional explosive device; water jet impact; blasting caps; IED neutralization

1. Introduction

The use of improvised explosive devices (IEDs) is one of the asymmetric actions employed by terrorists to cause destruction of material goods and loss of human lives [1-4]. An improvised explosive device is a device built in an artisanal manner, incorporating destructive, lethal, pyrotechnic, or incendiary materials, with the purpose of destruction, incapacitation, harassment, or diversion of attention. Usually, the IED refers to a system composed of an initiation mechanism, an explosive charge and a casing. It may incorporate military-grade materials but is generally designed with non-military components [5-7].

* Corresponding author
[1] PhD student, Military Technical Academy "Ferdinand I", Bucharest, Romania, e-mail: alexandru.casapu@mta.ro
[2] Prof., Civil and Military Engineering and Geomatics Department, Military Technical Academy "Ferdinand I", Bucharest, Romania, corresponding author, e-mail: marin.lupoae@mta.ro
[3] Prof., Mechatronics and Integrated Armament Systems Department, Military Technical Academy "Ferdinand I", Bucharest, Romania, eugen.trana@mta.ro
[4] PhD student, Military Technical Academy "Ferdinand I", Bucharest, Romania, e-mail: costin.berechet@mta.ro

The principle of IED neutralization consists of preventing its operation (detonation of the main explosive charge) and separating its component elements, in such a way that its initiation cannot be triggered by subsequent handling or interaction with the surrounding environment.

The main methods of neutralizing IEDs are: i) generating shockwaves through the impact between a projectile or a jet composed of various disrupting media and the IED; ii) generating shockwaves using lasers [8]; iii) generating very high temperatures using torches, resulting in the ignition and burning of the explosive substance [9].

This study focuses on neutralization methods based on generating shockwaves through the impact with a liquid jet. The main characteristic by which the performance of a neutralization system is assessed is its ability to induce a sufficiently high shock in the improvised explosive device to cause mechanical separation of its constituent components, while being limited to prevent the initiation of the explosive transformation of the active charge. In this regard, the performance criteria that need to be highlighted are the penetrating power and the ability to destroy a specific material (casing) and the mass, velocity, density, and kinetic energy of the projectile/jet. The shock transmitted to the initiation system and the main explosive charge is influenced by the type and material properties of the IED casing. Moreover, there is a notable lack of data in the technical literature regarding the interaction between water jets and IED casings, making this phenomenon one of the primary aspects examined in this study.

The propulsion systems of projectiles or jets can be divided into propulsion systems that use powder deflagration (disruptors) or explosive detonation (explosive propulsion systems). For the purpose of this study, the focus will be on explosive propulsion systems for liquid jets. These can be classified, based on the formation/action mode of the jet, into: a) cylindrical shape systems in a asymmetric sandwich configuration (propellant, explosive charge, liquid) with focalization and point-like action (liquid jet); b) unfocused systems (cylindrical system with axial charge); c) parallelepipedal systems with asymmetric closed sandwich charge and lamellar focalization, as shown in Fig. 1.

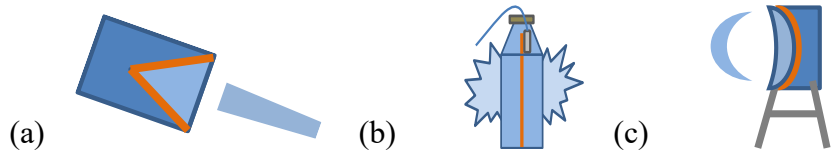

Fig. 1. Principles of operation of neutralization methods. (a) cylindrical shape; (b) unfocused systems; (c) parallelepipedal systems.

In military applications for IED neutralization, specially designed and constructed explosive propulsion devices are typically used. These devices generally result in the concentration of the liquid jet in the form of a liquid blade or

even unfocused systems (e.g., the Alford system [10]). However, there are also neutralization devices that utilize plastic containers, such as Mineral Water Bottles [11], with undirected effects. Although less effective than professional devices, they have the advantage of being cheaper and readily available.

Considering that the action of the neutralization system typically needs to target a specific area, this study analyzed the omnidirectional disruptor - OD, as shown in Fig. 1 (b). The study presents the results of experimental tests conducted to characterize ODs in terms of the propelled liquid jet velocity at distances typically used for these systems in relation to IEDs. Additionally, the behavior of casings made from various materials and with differing thicknesses under the impact of water jets was investigated. Moreover, the study presents the results of experimental and numerical tests conducted to determine the initiation of the blasting caps that can be equipped on IEDs by the aforementioned propulsion systems.

2. Materials and Methods

2.1 Theory of propulsion using explosives

Gurney [12] formulated a first model to predict the average initial velocity in terms of the charge to weight ratio of fragments created from a spherical or cylindrical metal case driven by an explosive, which has been further refined in many studies. The Gurney's method accuracy has been improved for low liner mass to explosive mass ratios by Hirsch's formulation [13], in the case of exploding cylinders and shells. Based on energetic considerations, Koch et. al. [14] linked the Gurney energy with the detonation velocity and the polytropic exponent developing equations that provide good estimates of Gurney velocity and energy, regardless of the experimental geometry. On the same energetic approach, Danel and Kazandjian [15] argued that the Gurney energy gives only a rough evaluation of experimental results. Furthermore, Keshavarz and Semnani [16] proposed a method to determine Gurney's velocity for new explosives that contain elements of carbon, hydrogen, nitrogen and oxygen by correlating the detonation Gurney velocity with explosive's elemental composition, loading density and condensed or gas phase heat of formation.

While the above-mentioned studies are based on using a solid shell, few studies are focused on the case of liquid enclosed explosive charge. As water is an incompressible medium, the wave results in the acceleration of the liquid, leading to a loss of shock wave energy as described by Milne et al. [17].

Loiseau et al. [18] performed a variety of experimental tests in which granular materials and liquids were explosively dispersed using spherical geometry charge. The maximum shell velocity was measured by videography and the results were compared with the standard Gurney model as well as with the porous Gurney

method developed by Milne [19]. He found that for different liquid materials or wetted systems, a maximum error of 15.6% and a mean error of 6.1% were obtained between the model and the experiments.

Tamba et al. [20] experimentally investigated the blast mitigation performances of spherical water layers, whose mass ratios to an explosive charge were 12.2, 44.5, and 107.2. They found a difference of 13% compared to the Gurney model.

The standard Gurney formulation is used in this study for the estimation of the velocity of the liquid jet propulsion. The initial velocity, which depends on the system configuration comprising the explosive mass (M_{ex}), water mass (M_w), can be calculated using Gurney's model.

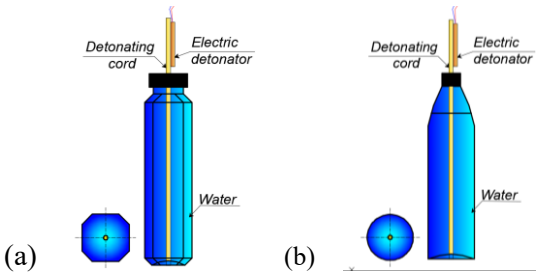

Fig. 2. Testing configurations for unfocused systems with axial charge (a) parallelepipedal shape; (b) cylindrical shape

In terms of the explosive charge-propelled mass configuration, the IED neutralization systems addressed in this study can be included in the category of cylindrical configuration, applicable to MWB-type systems with a cylindrical or parallelepipedal shape (Fig. 2), where the initial propulsion velocity can be calculated using Equation (1):

$$v_0 = \sqrt{2E} \cdot \left(\mu + \frac{1}{2}\right)^{-\frac{1}{2}} \tag{1}$$

where: $\sqrt{2E}$ represents the Gurney velocity and $\mu = \frac{M_w}{M_{ex}}$.

2.2 Numerical approach

2.2.1 Preprocessing

The explicit nonlinear finite element program Autodyn® software [21] was used to determine the velocity of jet-like structure of cylindrical and parallelepipedal water – explosive configuration. The numerical model is based on a 2D planar symmetrical geometry and the use of multi-material Euler part. Also, a 500 x 500 mm part of air was used, and the mesh dimension was set to 0.5 mm, as illustrated in Fig. 4 (a).

For the determination of water jet velocities, both parallelepiped-shaped and cylindrical containers were used, as shown in Fig. 3. For simulating the initiation of detonator caps upon impact with the water jet, only parallelepiped-shaped

containers were used, as experimental tests revealed better guidance of the water jets along the surface normal of the container. For both types of container shapes, the plastic casing (with thicknesses ranging from 0.18 to 0.25 mm) was not considered, as experimental tests showed that fragmentation of the container casing could generate fine-scale perturbations at the liquid interface [17]. The cylindrical containers had diameters of 62 mm for 0.5l, 78 mm for 1l, and 90 mm for 2l, while the cross-sectional dimensions for parallelepiped-shaped containers are presented in Fig. 3 (b).

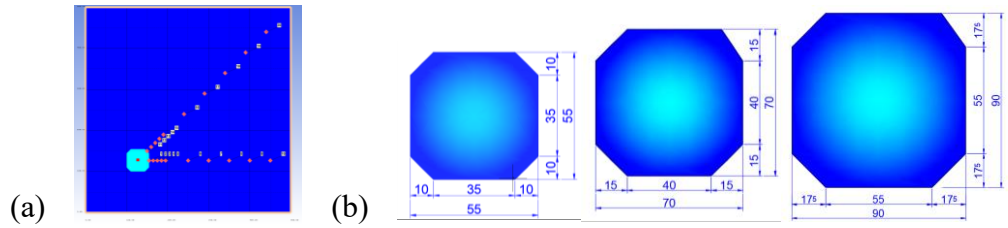

Fig. 3. Numerical modelling. (a) geometrical model for jet-like structure of velocity determination; (b) geometrical dimensions for containers

2.2.2 Material models

In numerical investigations of explosive detonation, it is common to utilize a specific equation of state (EOS) known as Jones-Wilkins-Lee (JWL) [22]. In fact, the JWL EOS is extensively employed to the extent that it has been implemented in almost all hydrocodes, and various forms of this equation can be found in the literature. Nevertheless, the most widely recognized form of the equation is the one representing a family of isentropes [23], which is demonstrated in Equation (8).

$$p(S,V) = Ae^{-R_1V} + Be^{-R_2V} + C^*(S)V^{-(\omega+1)}, \quad ((8)$$

where p is the pressure, S refers to the entropy per unit initial volume (s/v_0), V is the volume relative to the undetonated state (v/v_0), A, B, R_1 and R_2 are constant fitting parameters, ω is an assumed-constant material parameter (Grüneisen function), and $C^*(S)$ is a parameter dependent only upon the entropy S. The materials models that were used for the two types of numerical analyses were adopted from the library of the Autodyn® software.

3. Experimental procedure/setup

3.1 Measurements of water jet propulsion velocities

The used configuration for the experimental measurement of water jet propulsion velocities is shown in Fig. 4. The notations have the following meaning: 1) Explosive propulsion device; 2) Support wires for the explosive propulsion device; 3) Metal support frame; 4) Metal grids used for calibrating the image processing software of the high-speed camera; 5) Support for the initial positioning of the explosive propulsion device; 6) High-speed cameras.

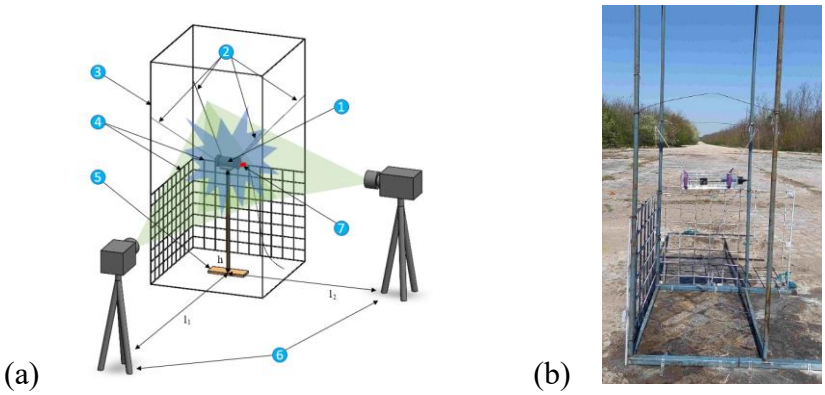

Fig. 4. The configuration for testing the propulsion velocities of liquid jets. (a) positioning of high-speed cameras (b) positioning of test containers

The decision was made to suspend the propulsion device in order to enable observation of water jet formation from all directions and eliminate any influence from the positioning surface. The velocity of the water jet was measured using two high-speed cameras (FASTCAM SA-Z type 2100K-C-128GB which was used for lateral view and was set to 30000 fps and FASTCAM SA-X2 type 1080K-C3, used for front view set to 12500 fps).

For the tests, two types of containers were used: cylindrical and parallelepiped plastic PET containers with volumes of 1l and 2l, as shown in Fig. 3. The PET containers were loaded with axial charges consisting of 3 passages (loops) of P20 detonating cord with a mass of 20 g/m, in the cylindrical axial configuration. The characteristics of the tested liquid jet propulsion devices are presented in Table 1.

Table 1

Information regarding PET configurations for experimental determination of liquid jet velocities

No.	Container shape	Container volume [l]	Explosive mass [g]		M_w/M_{ef}
			Effective[1]	Total[2]	
1.	parallelepipedal cylindrical	0.5	10.8	12.8	46
2.	parallelepipedal cylindrical	1	13.2	15.2	76
3.	parallelepipedal cylindrical	2	16.2	18.6	123

1) The effective explosive mass corresponds to the detonating cord that is placed between the water layers and contributes to the propulsion of the liquid jets.
2) The total mass is composed of the effective mass plus the detonating cord mass required for initiation.

3.2 Testing configuration for determining the initiation capability of detonator caps

A serie of tests were conducted with the target detonator positioned on a sandwich structure consisting of an aluminum plate (acting as a witness plate) and

a wooden support, as shown in Fig. 5. The blasting cap type used in these experiments, as donor and acceptor too, is based on 0.6 g PETN charge with a density of 1.75 gm/cm^3. The distances between the placement of the containers and the accepting detonators are provided in Table 4.

Fig. 5. (a, b) Configuration used for determining the minimum distance for positioning the neutralization charge relative to the (IED); (c) Testing configurations for assessing the material behavior

3.3 Configuration for testing casings made of different materials

A cube-shaped metallic structure with a 30 cm side length was employed, with its edges formed by L-shaped metal profiles measuring 30 mm each, as shown in Fig. 5 (c). One face of the cube was outfitted with a plate composed of either steel, Oriented Strand Board (OSB) wood, or solid transparent polycarbonate (TSPC). The study examined the jet's ability to penetrate casings fabricated from diverse materials and also its capacity to sever or detach the diverted electrical leads connected to the detonator. To emulate the detonator, an aluminum tube with a 7.5 mm diameter was employed; two copper conductors were crimped onto the tube and inserted via a rubber stopper which was firmly secured by compression within the metallic cube, as depicted in Fig. 5 (c). Two different volumes were used for the parallelepipedal container, 1 and 2 liters. In each case, 3 loops of detonating chord acted as the explosive charge, with 10.8 g effective explosive mass for the 1 liter case, and 13.2 g effective explosive mass for the 2 liter case.

4. Results and discussions

4.1 Water-jet formation

A series of representative images depicting the water propagation mode for the 2L parallelepiped and cylindrical shaped container is shown in Fig. 6

The use of two cameras filming from different directions allowed for a more accurate measurement of the water mass velocity compared to using only one camera. Consequently, the velocity of the water jet was measured on the lateral images, precisely in the intermediate region between the peaks.

The use of liquid-propelled explosive devices (LPEDs) for neutralizing IEDs requires positioning the neutralization system at distances of the order of tens

of centimeters from the IED. Placing the neutralization system in direct contact can lead to sympathetic initiation of the explosive charge in the IED, while positioning it too far may not achieve the desired effect due to dispersion of the liquid jets. The typical positioning distance ranges from 15 to 30 cm. Fig. 6 demonstrates that at distances up to 20 cm, the propelled water mass remains compact, although liquid jet structures are formed. When using explosive propulsion devices for IED neutralization, careful attention must be given to the variation in the mass of propelled liquid along the length of the container. Analysis of the images in Fig. 6 reveals that the water mass remains constant along the length of the container for both configurations, although the parallelepipedic configuration has more vertices than the cylindrical one.

Examining the distribution of the water mass at the cross-sectional level of the container (front view), it can be observed that from short distances (10 cm) onward, the liquid mass is distributed along the normals to the container faces. This characteristic becomes more apparent at greater distances, as shown in Fig. 7 (left - cylindrical shape, right - parallelepipedal shape). This means that, in terms of container shape, the parallelepipedic container propels a more directed liquid jet compared to the cylindrical container.

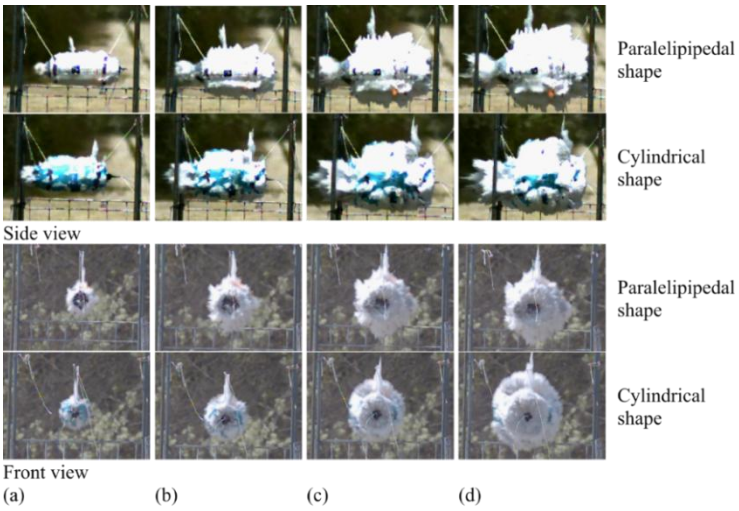

Fig. 6. The displacement of the water jet relative to top surface for the parallelepipedal and cylindrical shaped container: (**a**) d = 5 cm, (**b**) d = 10 cm, (**c**) d = 15 cm, (**d**) d = 20 cm

Fig. 7. The distribution of liquid jets as a function of container shape at a distance of 0.9 m

The variations in water jet velocities depending on the shape of the containers and the propelled water mass are presented in Fig. 8 and Table 2. At least 2 shots were performed for each configuration, and the velocities were measured from recorded images using a camera positioned perpendicular to the axis of the container (side view), in the middle portion of the container, and in the non-peak

threshold zone. It can be observed that the shape of the container (parallelepipedal or cylindrical) does not have a significant influence on the velocity values of the water jets, even though the velocity for the parallelepipedal shape is slightly higher than that for the cylindrical shape, as shown in Fig. 8.

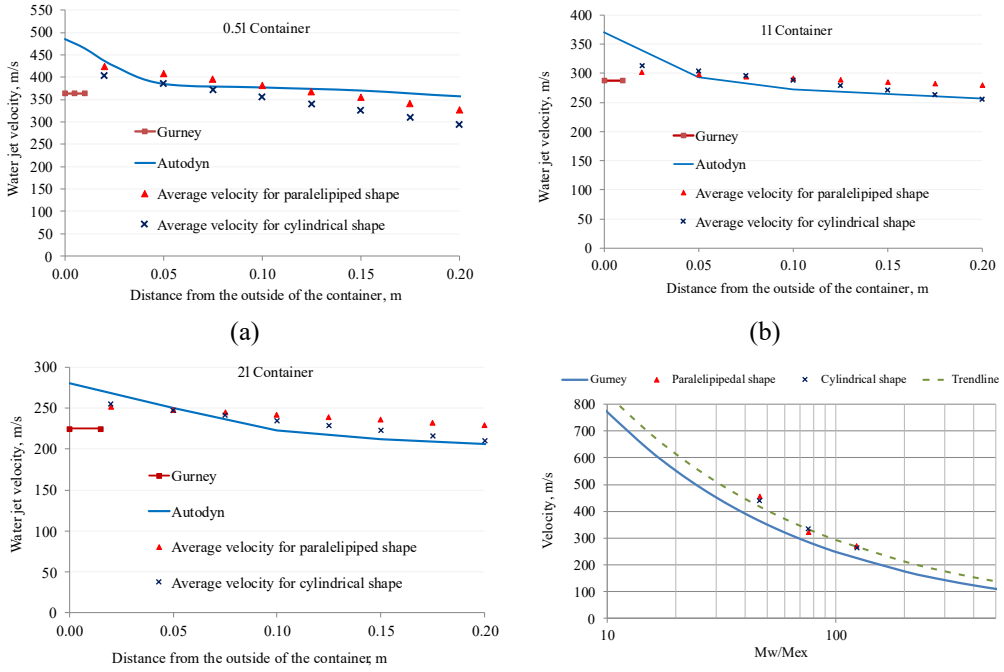

Fig. 8. The variation of water jet velocity with distance is dependent on the capacity of the container, its shape, and the Mw/Mex ratio. **(a)** Variation of water jet velocity for the 0.5 l container; **(b)** Variation of water jet velocity for the 1l container; **(c)** Variation of water jet velocity for the 2l container; **(d)** Variation of velocity as a function of the Mw/Mex ratio

The experimental maximum velocity of the water jets is reached between 2-3 cm from the outer casing and then decreases with increasing distance. The experimental maximum velocity values for the parallelepipedal shape of the container section are higher by 13-24% compared to the theoretical maximum velocity, while for the cylindrical shape, these differences range between 16 and 20%. For average values, these differences decrease to values ranging from 5-16% for the parallelepipedal shape and 9-13% for the cylindrical shape, which aligns with the literature findings. For spherical configurations, Loiseau et al. [18] found a maximum error of 15.6% and a mean error of 6.1% between the model and experiments for different liquid materials or wetted systems, while Tamba et al. [20] observed a difference of 13% between experiments and the Gurney model. The values of water jet velocities obtained experimentally are similar to those obtained by Ródenas-García et al. [24] following tests conducted on MWB-type devices.

Iorga et. al [25] provided a comparison between experimental data and numerical model for water-explosive experiments using the Gurney open sandwich configuration and showed a 10% averaged error between the two.

The graphical representation of the experimental water jet velocity as a function of the Mw/Mex ratio, Fig. 8 (d), shows that they follow the trend of Gurney's theoretical maximum velocity graph. The maximum values of water jets obtained through simulation are much higher than the theoretical maximum values, but at the distance where the experimental maximum values are recorded, it can be observed that the values obtained through simulation are quite close to the experimental ones and follow the same decreasing trend.

Table 2

The maximum values of water jet velocities as a function of the capacity and shape of the container

Container capacity, l	Mw/Mex	Maximum theoretical velocity, m/s	Maximum average experimental velocity, m/s			
			Paraleipipedal shape	Difference, %	Cylindrical shape	Difference, %
0.5	46	366	424	16	404	10
1	76	287	301	5	313	9
2	123	225	252	12	255	13

Considering the typical distance of placement for water jet propulsion-based IED neutralization systems (15-30 cm), it can be seen from the graphs in Fig. 8 (a), (b), (c) that at approximately 10 cm, the experimental velocity decreases to the value of the theoretical maximum velocity, and then the trend is a decreasing one, although not very steep. Even though the water jet velocity does not decrease significantly, the dispersion of the jets with increasing distance causes a reduced effect on the IED casing at placement distances larger than 25-30 cm, and the final result may not be as expected. The effect of the water jet is also influenced by the composition of the IED.

4.2 The effect on casings made from different materials

A comprehensive overview of the findings related to the performance of casings constructed from steel sheets, oriented strand board (OSB), and solid transparent polycarbonate (TSPC) is provided in Table 3. Detailed data analysis reveals that the response of these casings—regardless of their material composition and thickness—is significantly influenced by the extent of the surface area exposed to the liquid jets. In the experimental phase, square plates measuring 30 cm by 30 cm were utilized to test sheet materials such as steel, OSB, and TSPC. These plates were mounted on cubes featuring L-shaped profile edges, a configuration that was specifically designed to maintain uniform testing conditions across all specimens.

In tests involving water jet impacts on steel sheet containers, it was determined that the OD 1L and OD 2L devices are unsuitable for this application, despite the significant deformation observed in the sheet metal (see Fig. 9).

Table 3

The results regarding the behavior of casings

Material	Thickness [mm]	Effects	
		OD 1L	OD 2L
Steel sheet	0.8	Strong bending	Bending
	1.0	Bending	Bending
	1.5	Weak bending	Bending
	2.0	Weak bending	Bending
OSB	8	Breakage	Total breakage
	2x8	Breakage	Breakage / Partial breakage
	3x8	Breakage / perforation	Perforation
TSPC	5	Breakage	Breakage
	2x5	Partial breakage	Bending
	3x5	Partial breakage	Bending

The water jet forcefully propelled the metal sheets across the interior of the testing box, sending them a considerable distance from the casing. Additionally, for both the OD 1L and OD 2L devices, separation occurred only for a specific sheet thickness.

(a)  (b)  (c) 

Fig. 9. Material testing results (a) Metal sheet (0.8 mm); (b) OSB panels with a thickness of 3 × 5 mm; (c) TSPC panels with a thickness of 2 × 5 mm

For OSB panels (see Fig. 9), experiments showed that the water jets produced by both device types could perforate and fracture a casing constructed from three OSB panels, each 8 mm thick. Regarding the detachment of shunted wire leads from the cap, the findings indicate that this phenomenon is not directly linked to the jets' perforating or fracturing capabilities, with the omnidirectional 2L devices more frequently inducing such separation. Tests performed on TSPC panels (see Fig. 9) confirmed that the 1L and 2L omnidirectional devices are effective for this application, with a maximum panel thickness of 5 mm being manageable. TSPC material exhibits notable elasticity, causing casings made from it to undergo pronounced deformation under the influence of liquid jets, as shown in Fig. 9.

4.3 The effect on blasting caps

The results of experimental tests regarding sympathetic initiation of detonator caps due to the impact of water jets are presented in Table 4, and the effects produced by the impact of water jets on blasting caps are shown in Fig. 10.

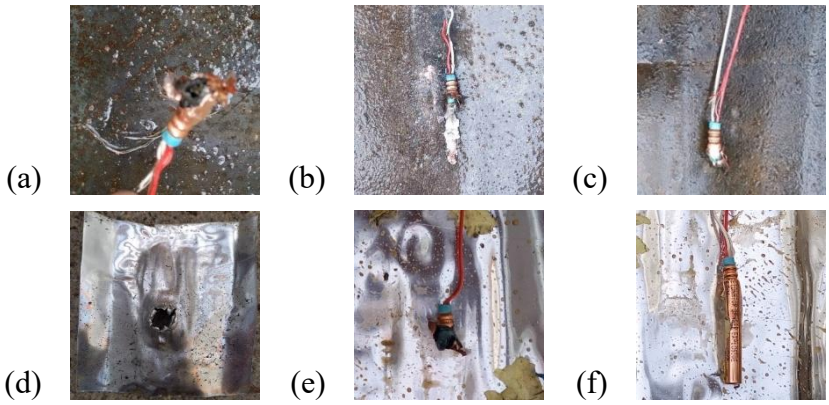

Fig. 10. The effects produced by the impact of water jets on detonator caps for the 1-liter plastic PET container. (a) Distance 4 cm, Steel witness plate – partial detonation; (b) Distance 5 cm, Steel witness plate – partial detonation; (c) Distance 10 cm, Steel witness plate – partial detonation; (d) Distance 10 cm, Aluminum witness plate – complete detonation; (e) Distance 10 cm, Aluminum witness plate – partial detonation; (f) Distance 15 cm, Aluminum witness plate – no detonation

When the water container and the acceptor charge are positioned in contact, the initiation of the acceptor charge occurs as a result of the shock wave action and the impulse transmitted by the explosion gases towards the liquid layer. The liquid layer will reduce the pressure in the shock wave front, but the magnitude of attenuation is difficult to predict. As the distance from the container increases, the overpressure in the shock wave front decreases significantly, even in the absence of the water layer, and the blasting cap initiation will only be influenced by the distance from the donor charge [26]. In the case of water layer, according to Pontalier et al. [27], for the 1-liter container configuration and a distance of 5 cm between it and the acceptor charge (Mw/Mex = 76 and scaled distance Z = 0.534 m/kg$^{1/3}$), the ratio between overpressure and incident pressure is sub unitary, meaning that the initiation of the acceptor charge is exclusively due to the action of the water jet.

Table 4

The results of experimental tests regarding the initiation of detonator caps by water jets propelled with explosives from 1 and 2-liter containers

Container capacity	Container – blasting cap distance, cm	Witness plate		Explosive reaction Y/N	
		Steel	Aluminum	Steel	Aluminum
1 liter	0	x	-	Y	-
	4	x	-	Y	-
	5	x	-	Y	-
	10	x	x	Y	Y
	10	x	x	N	N
	15	x	x	N	N
2 liters	0	x	-	Y	-
	5	x	-	N	-
	10	x	x	N	N

Complete detonation (Fig. 10 (d)) corresponds to the case where the main charge of the cap receives sufficient energy from the impact of the water jet to undergo complete detonation, resulting in rapid deformation and fragmentation of the cap's casing, as well as localized circular rupture of the witness plate. In this case, only the rubber sleeve with pieces of reinforcements, which ensures the sealing of the cap, can be recovered from the detonator cap.

In cases a, c, and e (Fig. 10 (a), (c), (e)), partial detonation occurs, where the explosive transformation of the cap's charge gives rise to local zones of high pressure, leading to ruptures in the cap's tube. Fragmentation occurs in larger pieces, which are often thrown at considerable distances. The case in Fig. 10 (f) corresponds to a situation where the transmitted energy to the charge is insufficient to initiate an explosive transformation mode. The effect on the detonator cap is deformation of the casing, usually in the middle or upper part, where there is no explosive material or where the explosive charge has a lower density, allowing the deformation of the cap. The case in Fig. 10 (b) corresponds to a situation where the cap's tube has been partially fragmented, with a fragment extending along the entire length of the cap's tube. The deformation mode of the tube indicates that an explosive transformation was initiated as a result of the impact, but it did not generate sufficient pressure to produce the effects of breaking the cap's casing into smaller fragments.

A sequence of images depicting the phases of action of a 1-liter omnidirectional water jet propulsion explosive device on acceptor detonator caps is presented in Fig. 11. After the initiation of the donor detonator cap and the detonator cord inside the 1-liter container (t = 0.1 ms), the detonation products from the donor cap and the detonator cord outside the container move towards the witness plate. The reflection of light from the fireball reaches the witness plate ahead of the detonation products and is reflected from it (t = 0.3 ms). The intensity and tonality of the light reflected from the witness plate indicate that initiation does not occur from the shock wave or explosion gases.

The action of the water jet on the acceptor cap can be observed at time t = 0.5 ms. At this time, the water jet has already reached the acceptor detonator cap for cases (a) and (b) in Fig. 11. The water jet prevents light reflection in case (a), and the area marked with a red color indicates the detonation of the acceptor detonator cap. In case (b), there are still reflections of light on the witness plate, at the top part, due to the inclination of the witness plate and the water jet hitting it first at the bottom, causing incomplete initiation of the explosive reaction (partial detonation) of the acceptor cap - the area marked with an orange color. In case (c), the water jet reaches the acceptor cap later, and the energy transmitted to the acceptor cap is insufficient to initiate its explosive reaction.

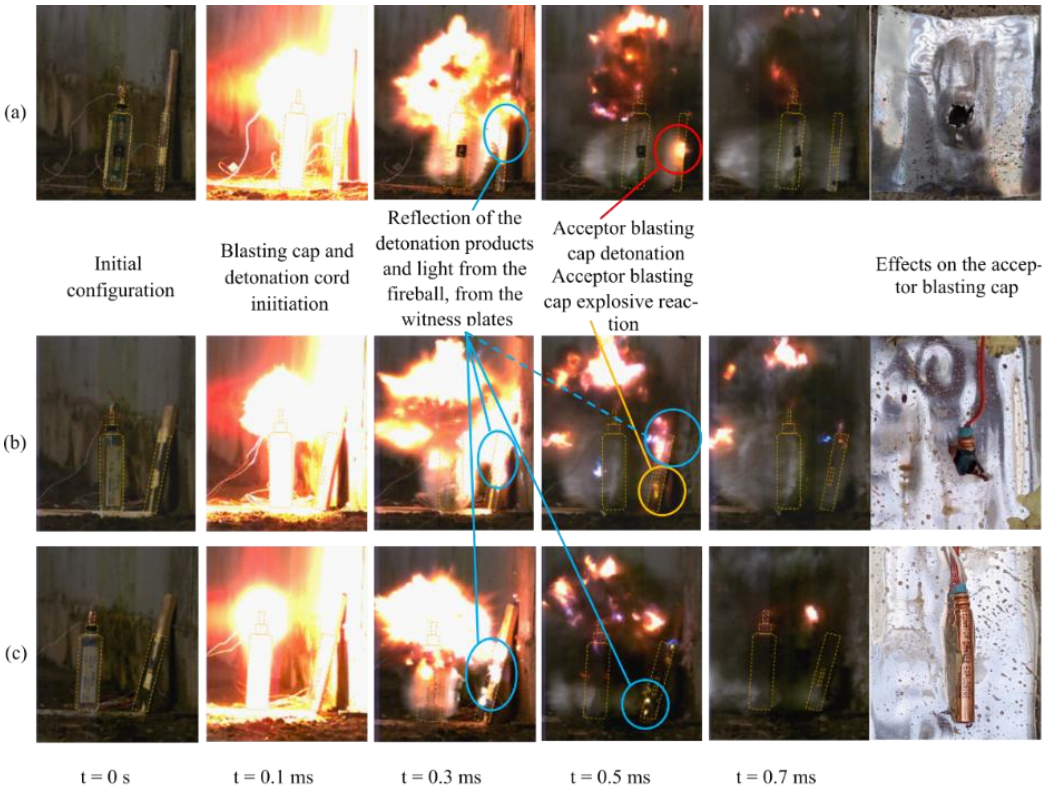

Fig. 11. Images of interaction between 1l omnidirectional explosive device and the acceptor blasting cap: (a) Distance 10 cm – complete detonation; (b) Distance 10 cm – explosive reaction (partial detonation); (c) Distance 15 cm – no reaction

5. Conclusions

This study focuses on providing insights into the experimental setup, measurement techniques, water jet formation, and the effects of water jets on IEDs casing and the initiation systems in their structure, mainly blasting caps.

Based on the given results of the water jet formation study, it can be stated up to a distance of 20 cm, the propelled water mass remains compact with the formation of liquid jet structures. Notably, the parallelepipedal container shape propels a more directed liquid jet compared to the cylindrical container shape. Although the container shape does not significantly impact water jet velocities, the experimental maximum velocities are slightly higher for the parallelepipedal shape compared to the theoretical maximum velocities. At placement distances beyond 25-30 cm, the dispersion of water jets diminishes their effect on the IED casing. The experimental velocities align closely with the values that can be found in the literature.

The experiments indicate that the efficacy of water jet neutralization devices is strongly influenced by the material properties of IED casings. For instance, while steel casings deformed considerably under jet impact, the OD 1L and OD 2L devices often failed to perforate them, especially when the steel was thicker. In contrast, OSB casings made from 8 mm panels consistently broke apart under the water jets. TSPC casings, with their high flexibility, bent significantly during testing, meaning the jets only worked on them up to a thickness of 5 mm.

The experimental findings reveal that the impact of water jets on blasting caps yields diverse effects. When the water jet imparts sufficient energy, complete detonation occurs, causing rapid deformation and fragmentation of the cap's casing, along with localized rupture of the witness plate. Partial detonation is characterized by the explosive transformation of the cap's charge, leading to high-pressure zones and ruptures in the cap's tube, with fragmentation of larger pieces. Deformation of the cap's casing occurs when the transmitted energy is insufficient for initiating explosive transformation. Based on the results obtained from the tests, it has been determined that the minimum distance for placing omnidirectional propulsion explosive devices in relation to IEDs is 15 cm.

Acknowledgments

This paper was partially supported by a grant of the Romanian Ministry of Innovation and Research, UEFISCDI, project number 33SOL/2021 within PNCDI III.

REFERENCES

[1] *Cuesta A, Abreu O, Balboa A, Alvear D* (2019) A new approach to protect soft-targets from terrorist attack. Safety Science 120:877-885. https://doi.org/10.1016/j.ssci.2019.08.019

[2] *Ramasamy A, Hill AM, Clasper JC* (2009) Improvised explosive devices: pathophysiology, injury profiles and current medical management. Journal of Army Medical Corps 155 (4):265-272. https://doi.org/10.1136/jramc-155-04-05

[3] *Arnold JL, Halpern P, Tsai MC, Smithline H* (2004) Mass casualty terrorist bombings: a comparison of outcomes by bombing type. Ann Emerg Med 43 (2):263-273. https://doi.org/10.1016/S0196-0644(03)00723-6

[4] *Golan R, Soffer D, Givon A, Peleg K* (2014) The ins and outs of terrorist bus explosions: Injury profiles of on-board explosions versus explosions occurring adjacent to a bus. Injury 45 (1):39-43. https://doi.org/10.1016/j.injury.2013.02.004

[5] Homeland Security. IED Attack: Improvised Explosive Devices. A fact sheet from the National Academies and Department of Homeland Security. Available online: https://www.dhs.gov/xlibrary/assets/prep_ied_fact_sheet.pdf . Accessed 08 January 2025

[6] *Gill P, Horgan J, Lovelance J* (2011) Improvised explosive device: the problem of definition. Stud. Conflict Terrorism 34:732-748. https://doi.org/10.1080/1057610X.2011.594946

[7] *Bevan, J* (2008) Conventional ammunition in surplus a reference guide. Small Army Survey: Geneva, Switzerland

[8] *Osterholz J, Lueck M, Lexow B, Wickert M* (2016) Neutralization of improvised explosive devices by high-power lasers: research results from the FP7 project ENCOUNTER. High-Power Lasers 2016: Technology and Systems. https://doi.org/10.1117/12.2241083

[9] *Divyakant P* (2009) Proper Usage of Torch Systems for In Situ Landmine Neutralization by Burning for Humanitarian Demining. The Journal of ERW and Mine Action 13(1):43.
[10] Alford Technologies (2021) https://www.explosives.net/cied-iedd. Accessed 23 June 2023
[11] Alford Technologies (2021) https://www.explosives.net/bottler. Accessed 23 June 2023
[12] *Gurney RW* (1943) The initial velocities of fragments from bombs, shell and grenades. Technical Report BRL-405, US Army Ballistic Research Laboratory. https://apps.dtic.mil/sti/citations/tr/ADA800105
[13] *Hirsch E* (1986) Improved Gurney Formulas for Exploding Cylinders and Spheres using "Hard Core" Approximation. Propellants, Explosives, Pyrotechnics 11(3):81-84. https://doi.org/10.1002/prep.19860110303
[14] *Koch A, Arnold N, Estermann MA* (2002) Simple Relation between the Detonation Velocity of an Explosive and its Gurney Energy. Propellants, Explosives, Pyrotechnics 27(6):365-368. https://doi.org/10.1002/prep.200290007
[15] *Danel JF, Kazandjian L* (2004) A Few Remarks About the Gurney Energy of Condensed Explosives. Propellants, Explosives, Pyrotechnics 29(5):314-316. https://doi.org/10.1002/prep.200400060
[16] *Keshavarz M, Semnani A* (2006) The simplest method for calculating energy output and Gurney velocity of explosives. Journal of Hazardous Materials 131(1-3):1-5. https://doi.org/10.1016/j.jhazmat.2005.09.004
[17] *Milne A, Longbottom A, Frost DL, Loiseau J, Goroshin S, Petel O* (2017) Explosive fragmentation of liquids in spherical geometry. Shock Waves 27(3):383-393. https://doi.org/10.1007/s00193-016-0671-y
[18] *Loiseau J, Pontalier Q, Milne AM, Goroshin S, Frost DL* (2018) Terminal velocity of liquids and granular materials dispersed by a high explosive. Shock Waves 28(3):473-487. https://doi.org/10.1007/s00193-018-0822-4
[19] *Milne AM* (2016) Gurney Analysis of Porous Shells. Propellants, Explosives, Pyrotechnics 41(4):665-671. https://doi.org/10.1002/prep.201600016
[20] *Tamba T, Sugiyama Y, Ohtani K, Wakabayashi K* (2021) Comparison of blast mitigation performance between water layers and water droplets. Shock Waves 31:89–94. https://doi.org/10.1007/s00193-021-00990-3
[21] ANSYS Inc (2013) AUTODYN User manual version 14.0.
[22] *Kubota S, Saburi T, Nagayama K* (2020) Unified Form EOS for Detonation Products Based on Relationship between Initial Density and Detonation Velocity. AIP Conference Proceedings 2272:030012. https://doi.org/10.1063/12.0000799
[23] *Seglets SB* (2018) An examination of the JWL equation of state. US Army Research Laboratory, ARL-TR-8403. https://apps.dtic.mil/sti/tr/pdf/AD1055483.pdf
[24] *Ródenas-García JF, Otón-Martínez RA, Sancho-Val J, de Francisco Ortiz O, Jiménez Pacheco R, Gil Garnacho I* (2023) Experimental Evaluation of the Factors That Influence Cylindrical Water Projection Devices against IEDs. Appl. Sci. 13:1167.
[25] *Iorga O, Munteanu M, Țigănescu T-V, Marin A, Grigoroiu O, Epure C*, Simulation and experiments regarding the formation of water jets using explosive charges U.P.B. Sci. Bull., Series D, Vol. 86, Iss. 4, 2024
[26] *Trană E, Lupoae M, Iftimie B, Casapu AC* (2022) Assessment of the Sympathetic Detonation of Blasting Caps. Appl. Sci. 12:12761. https://doi.org/10.3390/app122412761
[27] *Pontalier Q, Loiseau J, Goroshin S, Frost DL* (2018) Experimental Investigation of Blast Mitigation and Particle–Blast Interaction During the Explosive Dispersal of Particles and Liquids. Shock Waves 28: 489-511. https://doi.org/10.1007/s00193-018-0821-5